International Journal of Heat and Mass Transfer 180 (2021) 121802

Contents lists available at ScienceDirect

International Journal of Heat and Mass Transfer

journal homepage: www.elsevier.com/locate/hmt

Conditionally Exact Closed-Form Solution for Moving Boundary Problems in Heat and Mass Transfer in the Presence of Advection

Ankur Jain*, Mohammad Parhizi

Mechanical and Aerospace Engineering Department, University of Texas at Arlington, Arlington, TX, USA

ARTICLE INFO

Article history:
Received 27 May 2021
Revised 11 July 2021
Accepted 31 July 2021
Available online 9 August 2021

Keywords:
Moving Boundary Problems
Phase Change
Advection
Stefan Problem
Eigenvalue Expansion
Approximate Analytical Methods

ABSTRACT

Moving boundary problems occur in a variety of heat and mass transfer processes. While significant literature already exists on the mathematical analysis of such problems in the presence of diffusion, there is a lack of general solutions for problems in which advective transport of heat/mass due to fluid flow also occurs. This paper presents an error function based analytical solution for a one-dimensional phase change problem in the presence of advection with constant velocity. While this solution is not universally exact, however, a mathematical condition to ensure exactness of the solution is derived. Good agreement with numerical simulations, as well as with past work for special cases is shown. Even outside the condition to ensure exactness, the present method is shown to offer improved accuracy compared to other approximate analytical methods. In particular, the method offers greater accuracy at large value of the Stefan number, where other approximate analytical methods usually perform poorly. The impact of Peclet number that represents advection on the accuracy of the method is investigated. It is shown, as expected, that the $\sqrt{t}$ dependence of phase change front propagation is not valid in the presence of advection in general. This work improves the theoretical understanding of an important phase change problem, and may find applications in the design and optimization of engineering processes and systems involving phase change.

1. Introduction

Theoretical modeling of moving boundary problems is of much interest in heat and mass transfer [1,2]. Such problems occur commonly in solid-liquid phase change as well as in reacting systems, with the phase change front or the reaction front constituting a moving boundary. Phase change heat transfer problems occur in various engineering applications such as thermal energy storage [3], casting of metals [4], thermal management [5] and freezing of food [6]. A few examples of mass transfer problems involving a moving boundary include silicon oxidation in semiconductors [7], and growth of solid electrolyte interface (SEI) layer in Li-ion batteries [8]. A vast body of literature already exists on the theoretical analysis of such moving boundary problems [1,2].

In general, moving boundary problems are challenging to solve due to the non-linearity introduced by the unknown location of the phase change interface [1,9]. Exact solutions exist only for a limited number of simple problems [1,10,11]. For example, Stefan [12] presented an exact solution for a one-dimensional phase change problem in a semi-infinite domain subject to a constant temperature boundary condition. The single-phase Stefan problem assumes the initial phase to be at the melting temperature, so that heat transfer is limited only to the newly formed phase. Neumann [13] presented an exact solution for a more general problem, referred to as the Neumann or the two-phase problem in which, the initial phase is not at the melting temperature, and a temperature distribution exists in both phases during the phase change process. Such pure-diffusion problems are solved using the principle of self-similarity, which shows that the location of the phase change front is proportional to $\sqrt{\alpha t}$, where α is the thermal diffusivity of the newly formed phase. A key non-dimensional number in such problems is the Stefan number, *Ste*, which may be interpreted as the ratio of sensible heat to latent heat [1]. *Ste* is usually, but not always, small [14].

Due to the non-linearity of phase change problems in general, development of approximate analytical solutions and understanding the range of validity of such solutions is of much interest. For instance, quasi-stationary technique has been used to solve phase change problems [15,16]. This method assumes a steady-state temperature distribution in the newly formed phase. The integral method, originally proposed for boundary layer problems in fluid mechanics has also been employed extensively to solve vari-

* Corresponding author. 500 W First St, Rm 211, Arlington, TX, USA 76019 Ph: +1 (817) 272-9338
E-mail address: jaina@uta.edu (A. Jain).

https://doi.org/10.1016/j.ijheatmasstransfer.2021.121802
0017-9310/

Nomenclature

C	specific heat capacity ($Jkg^{-1}K^{-1}$)
k	thermal conductivity ($Wm^{-1}K^{-1}$)
L_{ref}	reference lengthscale (m)
$\mathcal{L}$	latent heat of phase change (Jkg^{-1})
Pe_j	Peclet number, $Pe_j = U_j L_{ref}/\alpha_L$, for j=L,S
Ste	Stefan number, $Ste = C_L(T_{ref} - T_m)/\mathcal{L}$
T	temperature (K)
V	flow velocity (ms^{-1})
x	spatial coordinate (m)
y	location of the phase change front (m)
$\bar{y}$	non-dimensional location of phase change front, $\bar{y} = y/L_{ref}$
t	time (s)
α	diffusivity (m^2s^{-1})
$\bar{\alpha}^2$	ratio of thermal diffusivities, $\bar{\alpha}^2 = \frac{\alpha_L}{\alpha_S}$
$\bar{k}^2$	ratio of thermal conductivities, $\bar{k}^2 = \frac{k_L}{k_S}$
ρ	density (kgm^{-3})
τ	non-dimensional time, $\tau = \frac{\alpha_L t}{L_{ref}^2}$
θ	non-dimensional temperature, $\theta_j = (T_j - T_f)/(T_{ref} - T_f)$, for j=L, S
ξ	non-dimensional spatial coordinate, $\xi = \frac{x}{L_{ref}}$
λ	non-dimensional eigenvalue

Subscripts

i	initial temperature
L	liquid phase
f	phase change temperature
ref	reference
S	solid phase
0	imposed temperature

ous phase change problems [17,18]. In this method, a polynomial form for the temperature profile within the newly formed phase is assumed. The governing equation is then integrated over the newly formed phase, resulting in an ordinary differential equation for the phase change front [20]. Perturbation method, an approximate analytical technique has also been used to solve various moving boundary problems such as Stefan problems with time-dependent boundary conditions [19-21]. In this method, the temperature profile is written as a power series of the Stefan number. Derivation of the solution using perturbation method is often mathematically complicated, especially if higher order terms are considered [4]. Variable eigenvalue technique has been also used to solve one-dimensional transient phase change problems [22].

A key drawback of most approximate analytical solutions is that the solutions are often valid only for small *Ste* or short times. Significant error may be encountered at large *Ste*. This is primarily due to the nature of assumptions underlying the approximate methods. Therefore, several numerical techniques have also been developed for solving phase change problems. Fixed-grid methods [23], variable-grid methods [23], front-fixing method [24], and the enthalpy method [25] are among the commonly used numerical techniques. Numerical methods have been used to address more complicated phase change problems involving higher dimensions [26,27], phase change over a temperature range [28] and temperature-dependent thermal properties [29].

Most of the previous literature on moving boundary problems considered diffusion as the only heat transfer mechanism [11]. However, in specific practical applications, heat transfer may also occur due to advection driven by fluid flow in the liquid phase, and possibly in the porous solid phase as well. Equivalent mass

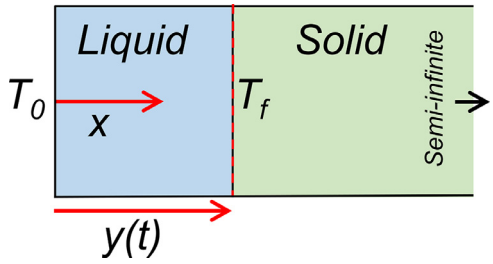

Fig. 1. Schematic showing the one-dimensional solid-to-liquid phase change problem considered here. Phase change is driven by both diffusion and advection. The opposite problem of freezing of a liquid, as well as mass transfer problems can be analyzed using the same framework.

transfer problems, involving advection of species towards or away from the reaction front due to fluid flow in addition to diffusion may also be important in practical applications. Accounting for advection is clearly important for accurate prediction of the evolution of the moving boundary in such problems, and traditional self-similarity based solution may not be valid when both diffusion and advection exist. While pure-diffusion phase change problems are well-studied [11], there is a relative lack of analytical models that account for the advection term in equations governing the phase change process. Most of the literature on buoyancy-driven flow during phase change rely on numerical solution of the energy and flow equations. Analytical treatment of problems with advection is available only for very specific problems [30-34]. For example, self-similarity based solution for one-dimensional convection-diffusion phase change problems have been derived under the specific assumptions of velocity [34] or imposed heat flux at the boundary [33] decaying as $1/\sqrt{t}$. Such self-similarity based solutions are not valid in general, or even for a commonly encountered constant velocity profile.

This paper derives an approximate analytical solution for a one-dimensional two-phase moving boundary problem in the presence of uniform advection. A solution for the temperature distribution is written in the form of error functions. A mathematical condition for exactness of the analytical solution is derived. Even outside of this range, results are shown to be in good agreement with numerical simulations, as well as with past results for special cases. In particular, results from the present work compare favorably with other approximate analytical methods, and offer much improved accuracy at large values of *Ste*. The next section defines the problem and presents a solution. Section 3 discusses a condition in which the results are exact. Further discussion of the results, including comparison with other approximate analytical techniques is presented in Section 4.

2. Problem definition

The problem considered here is shown schematically in Fig. 1. Consider a one-dimensional semi-infinite solid slab, initially at a uniform temperature T_i, which is lower than or equal to the phase change temperature T_f. Thermal conductivity, heat capacity and diffusivity are denoted by k, C and α respectively, and the liquid and solid phases are denoted by subscripts L and S, respectively. The latent heat for phase change is denoted by $\mathcal{L}$. At t=0, the phase change process is initiated by imposing a constant temperature T_0 ($>T_f$) on the boundary of the solid body, due to which, the solid begins to melt, and the phase change front propagates towards the right. Fluid flow with constant velocity U_L is assumed in the liquid phase. In case the solid itself is porous, there may be a fluid velocity U_S in the solid phase as well, assumed to be constant. In order to analyze the case of a non-porous solid, U_S can be simply set to zero. As the solid melts, thermal energy from the boundary is used

up to heat the liquid and, if $T_i<T_f$, solid phase, as well as drive the phase change process. If $T_i<T_f$, i.e., the solid is initially subcooled, there is a temperature gradient in both phases. In the absence of advection, this two-phase problem is often referred to as the Neumann problem. If $T_i=T_f$, the solid is initially at the melting temperature, and no heat transfer occurs into the solid. In the absence of advection, this one-phase problem is referred to as the Stefan problem. Both Neumann and Stefan problems have analytical solutions, in which, the location of the phase change front change is proportional to $\sqrt{t}$ [1].

While the problem discussed above pertains to the melting of a solid, the opposite problem – freezing of a liquid – can also be analyzed using the same framework. Further, mass transfer problems involving diffusion and advection of species through a layer before being consumed at a reaction front can also be analyzed similarly. Referring to Fig. 1, and assuming that all thermal properties are independent of temperature, energy conservation equations governing the temperature fields in the solid and liquid phases may be written as [1,9]

$$\frac{\partial^2 T_L}{\partial x^2} - \frac{U_L}{\alpha_L}\frac{\partial T_L}{\partial x} = \frac{1}{\alpha_L}\frac{\partial T_L}{\partial t} \tag{1}$$

$$\frac{\partial^2 T_S}{\partial x^2} - \frac{U_S}{\alpha_S}\frac{\partial T_S}{\partial x} = \frac{1}{\alpha_S}\frac{\partial T_S}{\partial t} \tag{2}$$

The two terms on the left hand sides represent heat transfer due to diffusion and advection, respectively. The usual boundary conditions associated with this problem are [1,9]

$$T_L = T_0 \text{at} \, x = 0 \tag{3}$$

$$T_L = T_S = T_f \text{at} \; x = \; y(t) \tag{4}$$

$$T_S = T_i \text{as} \; x \to \infty \tag{5}$$

where $y(t)$ represents the location of the phase change front.

In addition, the following equation may be written to represent the conservation of energy at the interface

$$-k_L\left[\frac{\partial T_L}{\partial x}\right]_{x=y} + k_S\left[\frac{\partial T_S}{\partial x}\right]_{x=y} = \rho_L \mathcal{L}\frac{dy}{dt} \tag{6}$$

The initial condition for the solid phase is

$$T_S = T_i \text{at} \; t = 0 \tag{7}$$

Non-dimensionalization is first carried out based on $\theta_j = \frac{T_j - T_f}{T_0 - T_f}$, where j=L,S, $\xi = \frac{x}{L_{ref}}$ and $\tau = \frac{\alpha_L t}{L_{ref}^2}$, where L_{ref} is a reference length. In the absence of a natural length scale in this problem, L_{ref} is arbitrary and is often assumed to be unity. This results in the following non-dimensional equations governing this problem

$$\frac{\partial^2 \theta_L}{\partial \xi^2} - Pe_L\frac{\partial \theta_L}{\partial \xi} = \frac{\partial \theta_L}{\partial \tau} \tag{8}$$

$$\frac{\partial^2 \theta_S}{\partial \xi^2} - Pe_S\frac{\partial \theta_S}{\partial \xi} = \bar{\alpha}^2\frac{\partial \theta_S}{\partial \tau} \tag{9}$$

$$\theta_L = 1 \text{at} \; \xi = 0 \tag{10}$$

$$\theta_L = \theta_S = 0 \text{at} \; \xi = \; \bar{y} \tag{11}$$

$$\theta_S = \theta_i \text{as} \; \xi \to \infty \tag{12}$$

$$\theta_S = \theta_i \text{at} \; t = 0 \tag{13}$$

$$-\left[\frac{\partial \theta_L}{\partial \xi}\right]_{\xi=\xi_{LS}} + \frac{1}{\bar{k}^2}\left[\frac{\partial \theta_S}{\partial \xi}\right]_{\xi=\xi_{LS}} = \frac{1}{Ste}\frac{d\xi_{LS}}{d\tau} \tag{14}$$

where $\theta_i = \frac{T_i - T_f}{T_0 - T_f}$ and $\bar{y} = \frac{y}{L}$ are the non-dimensional initial temperature and phase change front location, respectively. $Pe_j = \frac{U_j L}{\alpha_L}$ (j=L,S) is the Peclet number that represents the magnitude of advection relative to diffusion. $\bar{\alpha}^2 = \frac{\alpha_L}{\alpha_S}$ and $\bar{k}^2 = \frac{k_L}{k_S}$ represent the ratios of thermal diffusivities and thermal conductivities, respectively. Finally, $Ste = \frac{C_L(T_0 - T_f)}{\mathcal{L}}$ is the Stefan number. Note that $Pe_L = Pe_S = 0$ reduces this to a standard Neumann/Stefan problem in which, no advection occurs and heat transfer is driven only by diffusion. Well-known self-similarity based analytical solutions are available for these problems [1,4].

The liquid phase of the present problem with advection is considered first. Eq. (8) for the liquid temperature distribution is the convection-diffusion problem, which has been investigated widely [35-37], though not much in the context of phase change [30–32]. Based on past work on problems with fixed boundaries and no phase change [37,38], the following function satisfies Eq. (8) exactly:

$$f(\xi, \tau) = \frac{\text{erfc}\left(\frac{\xi - Pe_L\tau}{2\sqrt{\tau}}\right) + \exp(Pe_L\xi)\text{erfc}\left(\frac{\xi + Pe_L\tau}{2\sqrt{\tau}}\right)}{2} \tag{15}$$

where erfc is the complementary error function. Therefore, a general form for the liquid temperature distribution may be written as follows:

$$\theta_L = A + B\frac{\text{erfc}\left(\frac{\xi - Pe_L\tau}{2\sqrt{\tau}}\right) + \exp(Pe_L\xi)\text{erfc}\left(\frac{\xi + Pe_L\tau}{2\sqrt{\tau}}\right)}{2} \tag{16}$$

where A and B are coefficients that may be determined based on the boundary conditions.

Inserting Eq. (16) into Eqs. (11) and (12) and solving for A and B results in

$$A = \frac{-\hat{f}(\bar{y}, \tau)}{1 - \hat{f}(\bar{y}, \tau)} = \frac{-\frac{1}{2}\left[\text{erfc}\left(\frac{\bar{y} - Pe_L\tau}{2\sqrt{\tau}}\right) + \exp(Pe_L\bar{y})\text{erfc}\left(\frac{\bar{y} + Pe_L\tau}{2\sqrt{\tau}}\right)\right]}{1 - \frac{1}{2}\left[\text{erfc}\left(\frac{\bar{y} - Pe_L\tau}{2\sqrt{\tau}}\right) + \exp(Pe_L\bar{y})\text{erfc}\left(\frac{\bar{y} + Pe_L\tau}{2\sqrt{\tau}}\right)\right]} \tag{17}$$

$$B = \frac{1}{1 - \hat{f}(\bar{y}, \tau)} = \frac{1}{1 - \frac{1}{2}\left[\text{erfc}\left(\frac{\bar{y} - Pe_L\tau}{2\sqrt{\tau}}\right) + \exp(Pe_L\bar{y})\text{erfc}\left(\frac{\bar{y} + Pe_L\tau}{2\sqrt{\tau}}\right)\right]} \tag{18}$$

Where $\hat{f}(\bar{y}, \tau) = f(\xi = \bar{y}, \tau)$.

Note the time-dependence of A and B, due to which, the assumed form of the liquid temperature distribution may not exactly satisfy the governing energy equation, given by Eq. (8), unless Pe_L=0, or Pe_L scales as $1/\sqrt{\tau}$, in which case, $\bar{y}$ scales as $\sqrt{\tau}$, and therefore, A and B are pure constants. The important question of the validity of Eq. (16) as the solution for the liquid temperature distribution is addressed in section (3), where it is shown that under certain conditions, Eq. (16) satisfies Eq. (8) exactly. Comparison with numerical simulations discussed in Section 4 also demonstrates that this approximate analytical method offers excellent accuracy in a broad range of Ste and Pe numbers, including at large Ste.

Similar to the liquid problem, a general solution of the convection-diffusion equation in the semi-infinite solid domain, given by Eq. (9) can be written as [37,38]:

$$g(\xi, \tau) = \frac{\text{erfc}\left(\frac{\bar{\alpha}\xi - Pe_S^*\tau}{2\sqrt{\tau}}\right) + \exp\left(Pe_S^*\bar{\alpha}\xi\right)\text{erfc}\left(\frac{\bar{\alpha}\xi + Pe_S^*\tau}{2\sqrt{\tau}}\right)}{2} \tag{19}$$

where $Pe_S^* = \frac{Pe_S}{\bar{\alpha}}$. Therefore, the following form for the solid temperature distribution may be written:

$$\theta_S = C + D\frac{\text{erfc}\left(\frac{\bar{\alpha}\bar{\xi} - Pe_S^*\tau}{2\sqrt{\tau}}\right) + \exp\left(Pe_S^*\bar{\alpha}\bar{\xi}\right)\text{erfc}\left(\frac{\bar{\alpha}\bar{\xi} + Pe_S^*\tau}{2\sqrt{\tau}}\right)}{2} \tag{20}$$

Coefficients C and D may be determined using the boundary conditions, Eqs. (11) and (12), as follows:

$$C = \theta_i \tag{21}$$

$$D = \frac{-2\theta_i}{\text{erfc}\left(\frac{\bar{\alpha}\bar{y} - Pe_S^*\tau}{2\sqrt{\tau}}\right) + \exp\left(Pe_S^*\bar{\alpha}\bar{y}\right)\text{erfc}\left(\frac{\bar{\alpha}\bar{y} + Pe_S^*\tau}{2\sqrt{\tau}}\right)} \tag{22}$$

Note that if the solid is initially at the melting temperature, which is a commonly made assumption justified by the large latent heat of common materials, then $\theta_i = 0$, and therefore, $\theta_S = 0$, i.e., there is no heat transfer or temperature field in the solid.

Once expressions for θ_L and θ_S are available from Eqs. (16) and (20), respectively, the interface equation given by Eq. (14) may be used to derive an equation governing the phase change front location $\bar{y}$. Eqs. (16) and (20) are differentiated with respect to $\bar{\xi}$ at $\bar{\xi} = \bar{y}$, and inserted in Eq. (14) to result in the following ordinary differential equation for $\bar{y}$

$$\frac{d\bar{y}}{d\tau} = -\frac{Ste}{2}\left[-\frac{1}{\sqrt{\pi}\sqrt{\tau}}\left[\exp\left[-\left(\frac{\bar{y} - Pe_L\tau}{2\sqrt{\tau}}\right)^2\right] + \exp\left(\bar{y}Pe_L\right)\exp\left[-\left(\frac{\bar{y} + Pe_L\tau}{2\sqrt{\tau}}\right)^2\right]\right] + Pe_L erfc\left(\frac{\bar{y} + Pe_L\tau}{2\sqrt{\tau}}\right)\right] +$$
$$\frac{Ste\cdot\theta_i}{\bar{k}^2}\left[-\frac{\bar{\alpha}}{\sqrt{\pi}\sqrt{\tau}}\left[\exp\left[-\left(\frac{\bar{\alpha}\bar{y} - Pe_S^*\tau}{2\sqrt{\tau}}\right)^2\right] + \exp\left(\bar{\alpha}\bar{y}Pe_S^*\right)\exp\left[-\left(\frac{\bar{\alpha}\bar{y} + Pe_S^*\tau}{2\sqrt{\tau}}\right)^2\right]\right] + Pe_S^*\bar{\alpha}erfc\left(\frac{\bar{\alpha}\bar{y} + Pe_S^*\tau}{2\sqrt{\tau}}\right)\right] \tag{23}$$

An appropriate initial condition for Eq. (23) is that $\bar{y} = 0$ at $\tau = 0$. While analytical integration of Eq. (23) is not likely, it can be easily integrated numerically to provide the phase change front location as a function of time, and subsequently, the liquid and solid temperature distributions as well.

Note that in many cases, the solid is initially at the melting temperature, or the subcooling of the solid is neglected, because the heat needed for phase change is much greater than for sensible heating of the solid. In such a one-phase problem, the term containing θ_i in the right hand side of Eq. (23) may be ignored, resulting in significant simplification.

Further, note that setting $Pe_L = Pe_S = 0$ reduces Eq. (14) to the well-known Neumann ($\theta_i \neq 0$) and Stefan ($\theta_i = 0$) solutions of the pure-diffusion problems, in which the phase change front $\bar{y}$ scales as $\sqrt{\tau}$. In the more general case considered here, with constant advection velocity, the $\sqrt{\tau}$ scaling may not be valid any more, and $\bar{y}$ is obtained, in general, by solving Eq. (23). Numerical integration of Eq. (23) is quite straightforward since the derivative of $\bar{y}$ is provided explicitly. The scaling of $\bar{y}$ with τ in the advection problem is discussed in more detail in Section 4.

As discussed above, the liquid and solid temperature distributions given by Eqs. (16) and (20) may not satisfy the governing energy equation exactly, due to which, the solution derived here must, in general, be viewed as an approximate analytical solution of the problem. Section 3 analyzes the conditions in which the analytical solution is indeed exact. Further, the accuracy of the analytical solution derived in this section, and the dependence of the error on key non-dimensional parameters, such as *Ste* and *Pe* is discussed in Section 4.

The solution derived here is close to, but not a self-similarity solution. The existence of a self-similarity solution for the present problem is unlikely due to the existence of a length scale in the problem. Self-similarity solutions for similar problems [33,34] have been derived for very specific conditions, and not valid for generalized analysis presented here.

3. Conditions for exactness of the analytical solution

This section discusses the conditions in which the liquid and solid temperature distributions, given by Eqs. (16) and (20), respectively, satisfy the governing energy conservation equations exactly. Starting with the liquid temperature distribution, such a condition may be examined by inserting Eq. (16) into Eq. (8). This results in the following requirement

$$B\left(\frac{\partial^2 f}{\partial\bar{\xi}^2} - Pe_L\frac{\partial f}{\partial\bar{\xi}}\right) = B\frac{\partial f}{\partial\tau} + \frac{dA}{d\tau} + f\frac{dB}{d\tau} \tag{24}$$

where f, A and B are given by Eqs. (15), (17) and (18), respectively.

Note that the left hand side and the first term on the right hand side in Eq. (24) cancel each other out. Therefore, the requirement for the solution given by Eq. (16) to be exact may be written as

$$\frac{dA}{d\tau} + f\frac{dB}{d\tau} = 0 \tag{25}$$

Now, from Eq. (17), $A = 1 - B$. Further, since $\bar{y}$ itself is a function of τ, therefore,

$$\frac{dB}{d\tau} = \frac{1}{\left[1 - \hat{f}(\bar{y},\tau)\right]^2}\left[\frac{\partial\hat{f}}{\partial\bar{y}}\frac{d\bar{y}}{d\tau} + \frac{\partial\hat{f}}{\partial\tau}\right] \tag{26}$$

Therefore, the general requirement for exactness may be written simply as

$$\frac{1}{\sqrt{\pi}}\left[\exp\left(-\left(\frac{\bar{y} - Pe_L\tau}{\sqrt{\tau}}\right)^2\right)\left[\frac{\bar{y}' - Pe_L}{2\sqrt{\tau}} - \frac{\bar{y} - Pe_L\tau}{4\tau\sqrt{\tau}}\right]\right.$$
$$+\exp\left(\bar{y}Pe_L\right)\exp\left(-\left(\frac{\bar{y} + Pe_L\tau}{\sqrt{\tau}}\right)^2\right)\left[\frac{\bar{y}' + Pe_L}{2\sqrt{\tau}} - \frac{\bar{y} + Pe_L\tau}{4\tau\sqrt{\tau}}\right]$$
$$\left.\frac{\sqrt{\pi}}{2}Pe_L\bar{y}'\exp\left(\bar{y}Pe_L\right)\text{erfc}\left(\frac{\bar{y} + Pe_L\tau}{2\sqrt{\tau}}\right)\right] = 0 \tag{27}$$

When this condition is satisfied, Eq. (16) represents an exact solution for the liquid temperature distribution. Note that this statement pertains only to the governing energy conservation equation. It is possible, in general, for the error in predicting the phase change front location to be negligibly small even when Eq. (8) is not satisfied exactly, because the liquid temperature distribution appears in the ODE for $\bar{y}$ only as a derivative at $\bar{\xi} = \bar{y}$.

In order for Eq. (27) to hold, it is sufficient that $(\frac{\bar{y} - Pe_L\tau}{\sqrt{\tau}}) \gg 0$, because this results in the exponential and complementary error function terms in Eq. (27) to both be zero ($\exp(-x^2)$ and $\text{erfc}(x)$ are both zero for large x). Except when τ is unrealistically large, this condition is satisfied if

$$Pe_L << \frac{\bar{y}}{\tau} \tag{28}$$

Note that this is a sufficient, but not necessary condition for exactness. In other words, one may obtain good accuracy in phase

change front prediction even if Pe_L is not much smaller than $\frac{\bar{y}}{\tau}$, because of the exponential terms in Eq. (27) that decay very rapidly.

It is well known that deriving a bound for the error associated with approximate analytical solutions of phase change problems is not possible even for much simpler phase change problems [1]. However, an error analysis based on comparison with numerical simulations presented in Section 4 shows that, in general, the error is the least when Pe_L and Ste are both small. Section 4 also shows that this method incurs lower error compared to other approximate analytical methods, especially at large Ste.

A condition for exactness of the solid temperature distribution may be derived along similar lines. By inserting Eq. (20) in Eq. (9), the requirement for exactness may be written as

$$D\left(\frac{\partial^2 g}{\partial \xi^2} - Pe_S \frac{\partial g}{\partial \xi}\right) = \bar{\alpha}^2 \left(D\frac{\partial g}{\partial \tau} + g\frac{dD}{d\tau}\right) \tag{29}$$

where g, C and D are given by Eqs. (19), (21) and (22), respectively. Using the properties of g, and some mathematical rearrangement, it can be shown that the following condition ensures exactness:

$$\frac{1}{\sqrt{\pi}}\left[\exp\left[-\left(\frac{\overline{\alpha}\cdot\bar{y} - Pe_S^*\tau}{\sqrt{\tau}}\right)^2\right]\left[\frac{\overline{\alpha}\cdot\bar{y}' - Pe_S^*}{2\sqrt{\tau}} + \frac{\overline{\alpha}\cdot\bar{y} - Pe_S^*\tau}{4\tau\sqrt{\tau}}\right]\right.$$
$$+\exp\left(\overline{\alpha}\cdot\bar{y}Pe_S^*\right)\exp\left[-\left(\frac{\overline{\alpha}\cdot\bar{y} + Pe_S^*\tau}{\sqrt{\tau}}\right)^2\right]\left[\frac{\overline{\alpha}\cdot\bar{y}' + Pe_S^*}{2\sqrt{\tau}} - \frac{\overline{\alpha}\cdot\bar{y} + Pe_S^*\tau}{4\tau\sqrt{\tau}}\right]$$
$$\left.\frac{\sqrt{\pi}}{2}\overline{\alpha}\cdot\bar{y}'Pe_S^*\exp\left(\overline{\alpha}\cdot\bar{y}Pe_S^*\right)\mathrm{erfc}\left(\frac{\overline{\alpha}\cdot\bar{y} + Pe_S^*\tau}{2\sqrt{\tau}}\right)\right] = 0 \tag{30}$$

Finally, similar to the liquid problem, it can be shown that this condition may be satisfied if

$$Pe_S << \bar{\alpha}^2\frac{\bar{y}}{\tau} \tag{31}$$

This completes the set of requirements for the analytical solution derived here to be exact. Since $\bar{y}$ is expected to scale slower than linearly in time, therefore, for a given set of conditions, Eqs. (28) and (31) become more and more difficult to satisfy as τ increases. In other words, it is likely, based on the analysis above, that the method discussed here is exact at early times and may lose accuracy as time passes. In addition, the method is also expected to become less and less accurate as the Peclet number increases. In light of this discussion, a comparison of results from this method with numerical simulations may be helpful. This is presented in detail in Section 4.

4. Results and discussion

4.1. Comparison with self-similarity solutions and numerical simulations

It is of interest to compare the results from the present work with exact solutions available for special cases, as well as with numerical simulations for more general cases. A comparison with the exact Neumann solution in absence of advection is presented in Fig. 2. For a number of values of Ste, Fig. 2(a) plots the phase change front location as a function of time. Other parameters used for Fig. 2(a) are $\theta_i = -1.0$, $\bar{\alpha} = 1$, $\bar{k} = 1$. For the same parameters and with Ste=0.4, Fig. 2(b) plots the temperature distributions at three different times. Fig. 2(a) shows, as expected, rapid phase change propagation initially, followed by a slow down due to increased thermal resistance of the growing liquid layer. There is excellent agreement between the present work and the Neumann solution based on self-similarity. As Ste increases, so does the rate of phase change propagation, which is expected because Ste represents the magnitude of the temperature boundary condition that drives the phase change process. The propagation of phase change front with time is also seen in Fig. 2(b). Further, temperature distributions shown in Fig. 2(b) decay to a value of $\theta_i = -1.0$ at large ξ. Similar to Fig. 2(a), excellent agreement in the computed temperature distribution between the present work and the Neumann solution is observed in Fig. 2(b).

For a more general case with advection, a comparison of the method described in this work with numerical simulations is presented in Fig. 3. These numerical simulations are carried out using a variable timestep approach described in [4]. The governing equation and boundary conditions are discretized into equal spatial intervals Δx. The time intervals, Δt, on the other hand, do not have equal size and are determined in order that the phase change front propagates by an amount Δx after each timestep. The set of algebraic equations obtained from discretization are solved using an implicit finite difference scheme. Phase change front propagation with time for a one-phase problem is plotted in Fig. 3(a) for two different values of Pe_L, with Ste=0.13. Curves based on the model presented in this work are compared with numerical simulations. For the same conditions, Fig. 3(b) plots the temperature distribution in the liquid phase at $\tau = 1.4 \times 10^{-6}$ for the present method as well as numerical simulations. Figs. 3(a) and 3(b) show that the present work agrees almost exactly with numerical simulations at Pe_L=500. When Pe_L increases to 2000, there is slightly worse agreement, particularly at large times in Fig. 3(a). However, even at Pe_L=2000, the worst-case error is only 3.2%. The temperature plots in Fig. 3(b) show that there is greater curvature in the

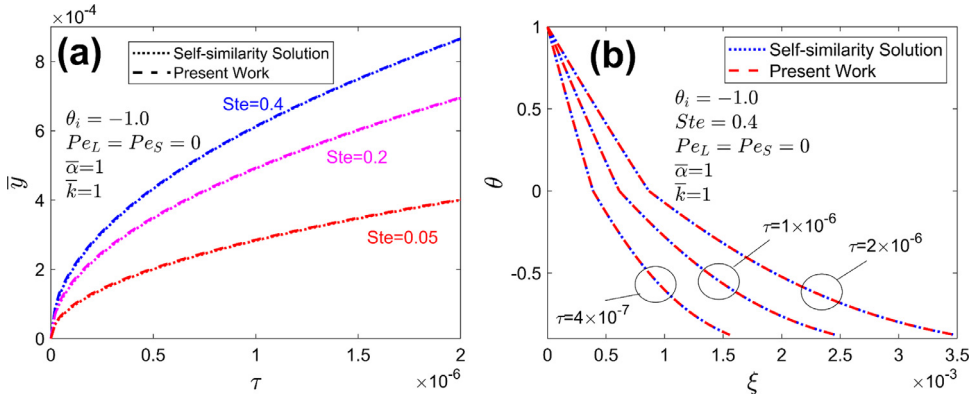

Fig. 2. Comparison of results with Neumann solution for the special case of no advection in both phases: (a) $\bar{y}$ as a function of τ for three different values of Ste; (b) Temperature vs ξ at three different times for $Ste = 0.4$. Other problem parameters are $Pe_L = 0$, $Pe_S = 0$, $\theta_{in} = -1.0$, $\overline{\alpha} = 1$; $\overline{k} = 1$.

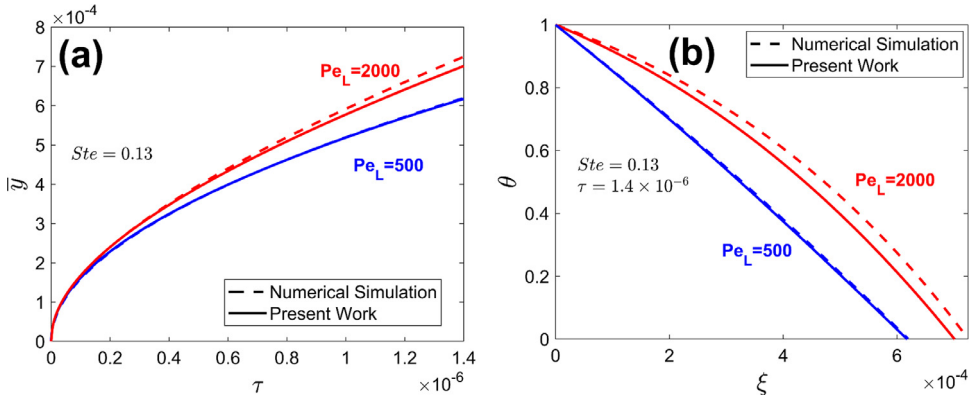

Fig. 3. Comparison of results with finite-difference simulations for a one-phase problem with advection: (a) Phase change front $\bar{y}$ as a function of τ; (b) Temperature distribution in liquid phase at $\tau = 1.4 \times 10^{-6}$. A value of $Ste = 0.13$ is used. Two different values of Pe_L are considered.

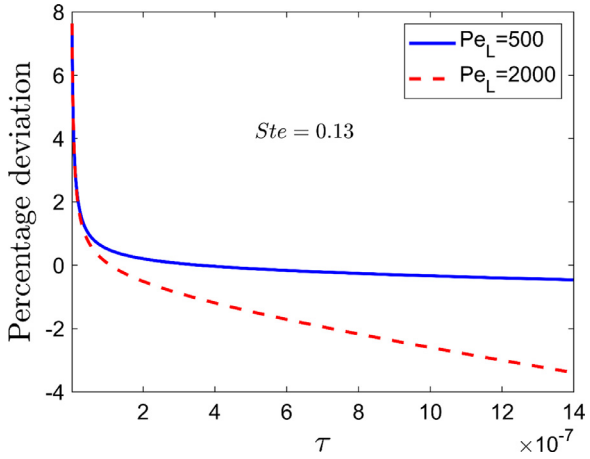

Fig. 4. Percentage deviation of the present work from numerical simulations as a function of τ during the phase change process for the two values of Pe_L considered in Fig. 3. All other parameters are the same as in Fig. 3(b).

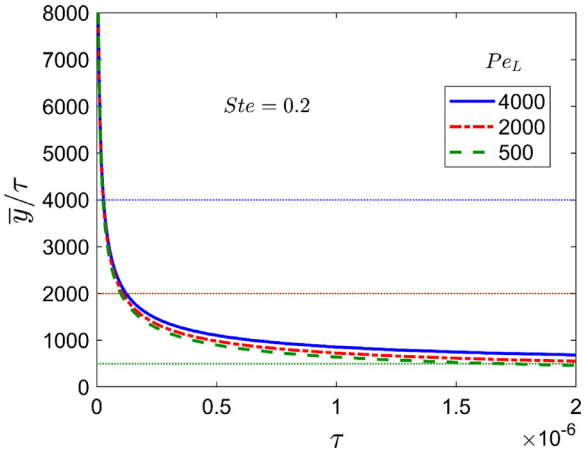

Fig. 5. Plot of $\bar{y}/\tau$ as a function of τ during the phase change process for the three values of Pe considered in Fig. 3. All other parameters are the same as in Fig. 3(b).

temperature distribution at large Pe_L, which is well-captured by the present method. These results demonstrate the accuracy of the analytical method discussed in Section 2.

Fig. 4 plots the deviation in the analytical method compared to numerical simulations as a function of time for a representative one-phase problem considered in Fig. 3. The deviation is defined in terms of phase change front location as a function of time, and is positive or negative if the model prediction is greater or smaller than the numerical simulation result. The deviation is somewhat large at very early times, most likely because of the small value of $\bar{y}$ at early times, which may amplify numerical computational error. For most of the time duration, the error is quite small, particularly for Pe_L=500, in which case, the error is nearly zero. This is consistent with Eq. (28), based on which, the analytical method is expected to be exact for longer times when Pe_L is small. For Pe_L=2000, the error gradually increases in magnitude with time, which is also consistent with the analysis presented in Section 3.

4.2. Error analysis and comparison with other approximate methods

As discussed in Sections 2 and 3, the analytical method described in Section 2 is exact under conditions given by Eqs. (28) and (31). For a one-phase problem with Ste=0.2, Fig. 5 plots $\bar{y}/\tau$ as a function of τ for three different values of Pe_L. According to Eq. (28), $\bar{y}/\tau$ must be much larger than Pe_L in order to ensure exactness of the method. Fig. 5 shows that $\bar{y}/\tau$ reduces sharply at first, and then plateaus out as τ increases. The curves shown in Fig. 5 appear to be nearly invariant of the value of Pe_L. For the three cases considered in Fig. 5, the corresponding Pe_L are indicated on the y axis. This shows that the analytical method is accurate for much longer time at small values of Pe_L than at larger values. Note that even outside the theoretical limit for exactness indicated by Eq. (28), the analytical method offers very small error, as shown in Figs. 3 and 4.

It is instructive to compare the analytical method described in this work with other approximate analytical methods for phase change problems. Three representative one-phase problems are solved using a number of methods, and results are summarized in Fig. 6, in terms of phase change front propagation as a function of time. In addition to numerical simulations and the analytical method described in this work, results from quasistationary, eigenfunction expansion and heat integral methods are also shown in Fig. 6. The quasistationary method determines the phase change front based on an assumed quasistationary temperature distribution in the newly formed phase [15]. The eigenfunction expansion method solves the transient heat equation in the liquid phase to determine the nature of phase change front propagation [39]. Finally, the heat integral method assumes a second-order polynomial form for the temperature distribution, based on which, the phase change front location is determined [4].

Three different sets of Pe_L and Ste values are considered. In the first set, Pe_L=500 and Ste=0.13 are both relatively low. In the second set, a higher value of Pe_L is considered while holding Ste at the same value. Finally, in the third set, Ste is increased while keeping

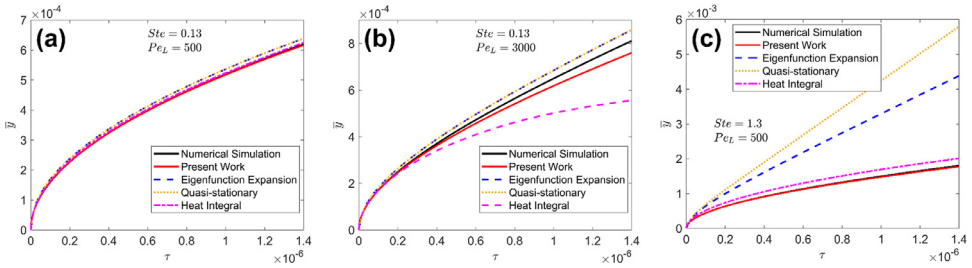

Fig. 6. Comparison of results from present work with other approximate analytical methods for a one-phase problem ($Pe_S = 0$): Phase change front $\bar{y}$ as a function of τ computed by the present work and three other approximate methods for (a) $Ste = 0.13$ and $Pe_L = 500$; (b) $Ste = 0.13$ and $Pe_L = 3000$; (c) $Ste = 1.3$ and $Pe_L = 500$. Results from a numerical simulation are also shown for comparison.

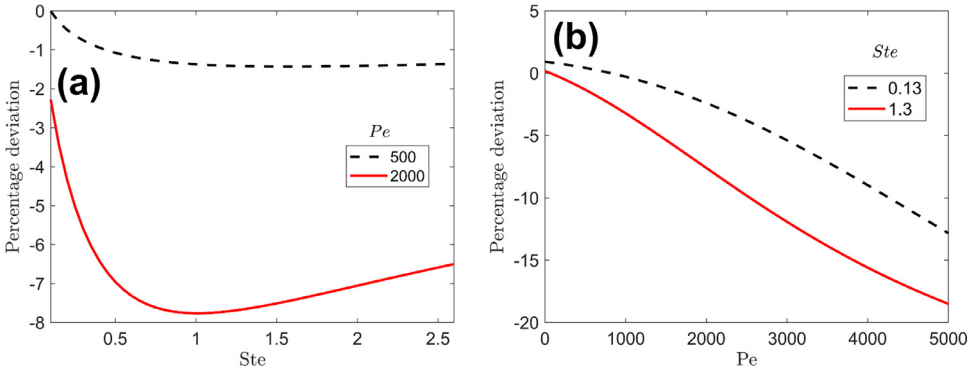

Fig. 7. (a) % deviation between the analytical method and numerical simulations (a) as a function of *Ste* for two fixed values of *Pe*; (b) as a function of *Pe* for two fixed values of *Ste*. Deviation is computed on the basis of predicted temperature at $\tau = 1.4 \times 10^{-6}$ compared to numerical simulation results.

Pe_L at the same value. Results for the three sets are summarized in Figs. 6(a)-(c), respectively. When Pe_L and *Ste* are both relatively small, each of the approximate analytical methods offer good accuracy, as shown in Fig. 6(a). At large Pe_L (Fig. 6(b)), the heat integral method performs poorly, while the performance of present work is comparable to that of quasistationary and eigenfunction expansion methods. At large *Ste* (Fig. 6(c)), the present method performs much better than all other methods considered here. In summary, the present method offers close agreement with the numerical simulation results in all conditions analyzed in Figs. 6(a)-(c), and performs much better than other methods. In contrast, the heat integral method works reasonably well for large *Ste*, but poorly for large Pe_L, whereas the quasi-stationary and eigenfunction expansion methods are reasonably accurate at large Pe_L, but very poor at large *Ste*. The good performance of the present method at large *Ste* is particularly remarkable because most approximate analytical methods for phase change heat transfer lose accuracy at large *Ste* [1]. The good performance of the present method at large *Ste* may be because the criteria for exactness of the present method is more directly related to Pe_L than to *Ste*, as shown in Eq. (28).

The accuracy of the analytical method is further evaluated as a function of Stefan and Peclet numbers, the two key parameters that represent the boundary condition and advection (relative to diffusion), respectively. Fig. 7(a) plots the deviation between the present method and numerical simulations for the predicted phase change front location at $\tau = 1.4 \times 10^{-6}$ as a function of *Ste* for a one-phase problem. Curves are plotted for two values of Pe_L. Results indicate that when Pe_L is relatively small, the deviation is also quite small. At Pe_L =2000, the deviation is larger, but still within 8%, even for large values of *Ste*. Fig. 7(a) shows that as *Ste* increases, the magnitude of the deviation peaks and then actually reduces at greater *Ste*. Most approximate analytical methods do not perform well at large *Ste* [1], which is why, the good performance of the present method at large *Ste* is remarkable. Fig. 7(b) presents a similar analysis of the dependence of the deviation on Pe_L, while *Ste* is held constant. This plot shows that the magnitude of the deviation grows monotonically with Pe_L, and is somewhat less sensitive to the value of *Ste*. As Pe_L increases, so does the deviation. However, as discussed in Fig. 6, the worst-case error for the present method is still much lower than the error incurred in other approximate analytical methods, which perform poorly when *Ste* and/or Pe_L is large.

4.4. Effect of diffusion and advection on phase change propagation

The effect of key non-dimensional parameters on the phase change process is examined next. Fig. 8 plots the nature of phase change front propagation with time for different values of Peclet number. The two-phase Neumann problem and one-phase Stefan problem are considered in Figs. 8(a) and 8(b), respectively. In each case, $\bar{y}$ is plotted as a function of τ and *Ste* is held constant at *Ste*=0.4. The no-advection Neumann and Stefan solutions are also shown in Figs. 8(a) and 8(b), respectively, for comparison. For the Neumann problem, other parameters are $\theta_i = -1.0$, $\bar{\alpha} = 1$, $\bar{k} = 1$. Fig. 8(a) shows that as $Pe_L(=Pe_S)$ increases, the phase change front propagates faster and faster. This is primarily because of greater advection of heat into the liquid phase, and therefore, greater liquid temperature, at larger values of Pe_L. At large times, phase change propagation slows down, but not as much as the classical zero-advection Neumann problem does. Similar observations can also be made for the one-phase Stefan problem shown in Fig. 8(b). Phase change propagation occurs faster in the Stefan problem than in the Neumann problem because of the additional energy needed to heat up the subcooled solid phase in the Neumann problem.

The effect of *Ste* on phase change propagation is presented in Fig. 9. Here, the Peclet number is held constant at Pe_L=Pe_S=1000. $\bar{y}$ is plotted as a function of τ for the Neumann and Stefan problems in Figs. 9(a) and 9(b), respectively for multiple values of *Ste*. These plots show that for both Neumann and Stefan problems, the larger the value of *Ste*, the faster is the propagation of phase change.

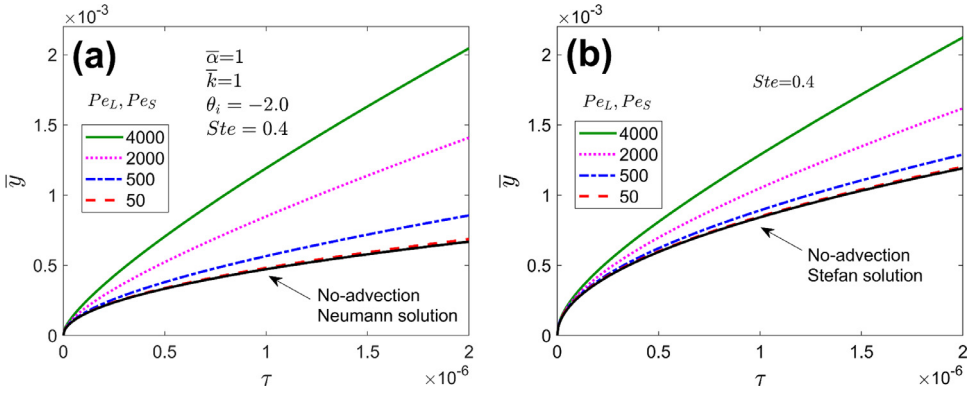

Fig. 8. Plots showing the impact of advection on phase change propagation: Phase change front $\bar{y}$ as a function of τ for three different values of $Pe_L = Pe_S = Pe$ for (a) two-phase problem ($Ste = 0.4$; $\theta_{in} = -2.0$; $\overline{\alpha} = 1$; $\overline{k} = 1$); (b) one-phase problem ($Ste = 0.4$). The self-similarity based exact solution for the no-advection case is also plotted for comparison.

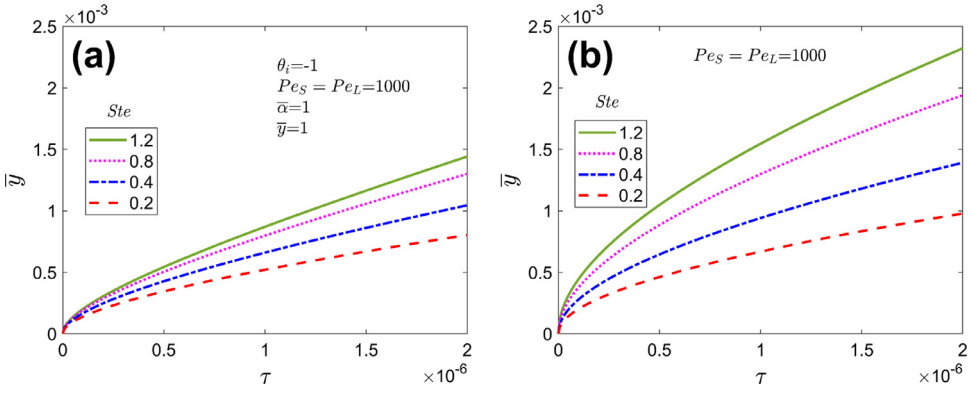

Fig. 9. Effect of the Stefan number on phase change propagation: Phase change front $\bar{y}$ as a function of τ for different values of Ste for (a) two-phase problem, with $Pe_L = Pe_S = 1000$; $\theta_{in} = -2.0$; $\overline{\alpha} = 1$; $\overline{k} = 1$; (b) one-phase problem, with $Pe_L = Pe_S = 1000$.

This is because Ste is related to the magnitude of the temperature boundary condition that drives the phase change process. In general, for the same values of Ste and Pe, phase change propagation is slower for the Neumann problem than the Stefan problem due to the need to heat up the subcooled solid in the Neumann problem.

Finally, the scaling of $\bar{y}$ with time for the phase change problem with advection is examined and compared with the zero-advection Neumann problem, in which, $\bar{y}$ grows proportional to $\sqrt{\tau}$. It is instructive to determine if a similar power scaling also exists in the presence of advection. Note that since diffusion and advection scale as $\sqrt{\tau}$ and τ, respectively, and since diffusion and advection both occur in the present problem, therefore, a scaling of τ^a, where $0.5<a<1$ may be expected. In order to investigate this systematically, $\log(\bar{y})$ is plotted as a function of $\log(\tau)$ in Fig. 10 for a number of different values of $Pe_L(=Pe_S)$. On a $\log(\bar{y})$-$\log(\tau)$ plot, the pure-diffusion Neumann solution appears as a straight line with a slope of 0.5, as shown in Fig. 10. Curves at different values of Pe_L shown in Fig. 10 exhibit a slope close to 0.5 at small times, but as time increases, the slopes in these curves also go up. Due to the increasing slope with time in the presence of advection, it is not possible to prescribe a uniform power law relationship between $\bar{y}$ and τ throughout the time period. This is likely because in this case, both diffusion and advection contribute towards the growth of the phase change front. At small times, diffusion contributes towards heat transfer to the phase change front – resulting in a slope close to 0.5 at small times – and as time increases, advection becomes more and more dominant, resulting in ever-increasing slope of the $\log(\bar{y})$-$\log(\tau)$ curve. Consistent with the nature of advection, the larger the value of Pe_L, the larger is the slope. Finally, it is seen from Fig. 10 that the slope never exceeds 1.0, which is also consistent with the linear nature of advection due to fluid flow.

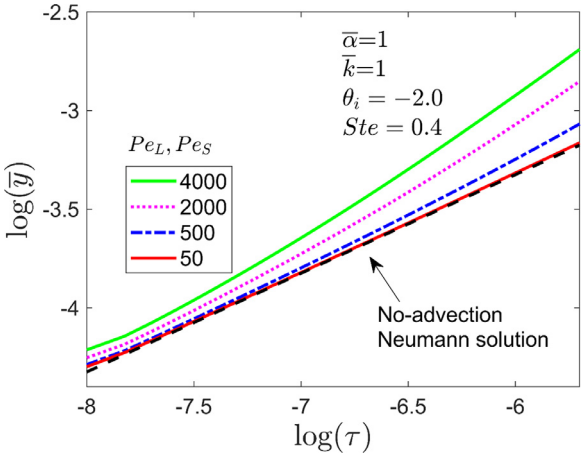

Fig. 10. $\bar{y}$ vs τ on a logarithmic scale to understand the scaling of $\bar{y}$ for multiple values of Peclet number. Problem parameters are the same as the two-phase problem considered in Fig. 8(a). The $\bar{y} = 2\lambda\sqrt{\tau}$ solution corresponding to the Neumann solution without advection is also plotted for comparison.

5. Conclusions

Mathematical modeling of phase change heat transfer is important for the design and optimization of a variety of practical engi-

neering systems. Such models are also helpful in analyzing mass transport problems involving a reaction front, such as oxidation of Silicon wafers and passivation layer formation in Li-ion cells. While phase change heat transfer with pure diffusion has been sufficiently analyzed in the past literature, there is relatively lesser work on analytical solutions for problems in which diffusion and advection both exist and together drive the phase change front propagation. The present work contributes towards addressing this gap in the literature.

While the analytical solution derived in this work is, in principle, not exact, nevertheless, it is shown that its performance compares very well with other approximate analytical techniques. Particularly, at large *Ste*, the method retains reasonable accuracy, whereas other methods are quite inaccurate. An analytical condition which, when satisfied, ensures exactness of the solution is also derived.

It is important to be aware of key limitations of the present work. It may not be applicable for problems where natural convection in the fluid or temperature-dependent thermal properties play a key role. Further, the method is limited only to one-dimensional heat and fluid flow with constant velocity. Finally, in some applications, phase change occurs over a temperature range, such as alloys, which is not accounted for by the model presented here.

In addition to improving our theoretical understanding of phase change heat transfer, it is expected that the mathematical models developed in this work may also aid in design and optimization of practical phase change based thermal management and energy storage systems.

Declaration of Competing Interest

The authors declare that they have no known competing financial interests or personal relationships that could have appeared to influence the work reported in this paper.

CRediT authorship contribution statement

Ankur Jain: Conceptualization, Methodology, Formal analysis, Validation, Investigation, Data curation, Supervision, Project administration, Writing – original draft, Writing – review & editing. **Mohammad Parhizi:** Conceptualization, Methodology, Validation, Data curation, Writing – original draft, Writing – review & editing.

Acknowledgments

This material is based upon work supported by CAREER Award No. CBET-1554183 from the National Science Foundation.

References

[1] V. Alexiades, Mathematical modeling of melting and freezing processes, CRC Press, 1992.
[2] V.J. Lunardini, Heat transfer with freezing and thawing, Elsevier, 1991.
[3] A. Mostafavi, M. Parhizi, A. Jain, Semi-analytical thermal modeling of transverse and longitudinal fins in a cylindrical phase change energy storage system, International Journal of Thermal Sciences 153 (2020) 106352.
[4] D.W. Hahn, M.N. Özışık, Heat conduction, 3rd ed., Wiley, Hoboken, N.J., 2012 p. 1 online resource (746 p.).
[5] M. Parhizi, A. Jain, Analytical modeling and optimization of phase change thermal management of a Li-ion battery pack, Applied Thermal Engineering 148 (2019) 229–237, doi:10.1016/j.applthermaleng.2018.11.017.
[6] J. Mannapperuma, R.P. Singh, Prediction of freezing and thawing times of foods using a numerical method based on enthalpy formulation, Journal of Food Science 53 (2) (1988) 626–630.
[7] B.E. Deal, A. Grove, General relationship for the thermal oxidation of silicon, Journal of Applied Physics 36 (12) (1965) 3770–3778.
[8] H.J. Ploehn, P. Ramadass, R.E. White, Solvent Diffusion Model for Aging of Lithium-Ion Battery Cells, Journal of The Electrochemical Society 151 (3) (2004), doi:10.1149/1.1644601.
[9] L. Rubinšteĭn, The Stefan problem, 1st, American Mathematical Soc., 1971.
[10] A. Mori, K. Araki, Methods for analysis of moving boundary-surface problem, International Chemical Engineering 16 (4) (1976) 734–744.
[11] D.A. Tarzia, A bibliography on moving-free boundary problems for the heat-diffusion equation, The Stefan and related problems, MAT-Serie A 2 (2000).
[12] J. Stefan, Über die Theorie der Eisbildung, insbesondere über die Eisbildung im Polarmeere, Annalen der Physik und Chemie 42 (1891) 269–286.
[13] B. Riemann, H. Weber, Die partiellen Differential-gleichungen der mathematischen Physik: nach Riemanns' Vorlesungen, in: 5. Aufl. bearb, F. Vieweg und Sohn, 1912.
[14] S.W. McCue, B. Wu, J.M. Hill, Classical two-phase Stefan problem for spheres, Proceedings of the Royal Society A: Mathematical, Physical and Engineering Sciences 464 (2096) (2008) 2055–2076.
[15] A. Solomon, D. Wilson, V. Alexiades, The quasi-stationary approximation for the Stefan problem with a convective boundary condition, International Journal of Mathematics and Mathematical Sciences 7 (3) (1984) 549–563.
[16] A. Stamatiou, S. Maranda, F. Eckl, P. Schuetz, L. Fischer, J. Worlitschek, Quasi-stationary modelling of solidification in a latent heat storage comprising a plain tube heat exchanger, Journal of Energy Storage 20 (2018) 551–559.
[17] R. Tien, G. Geiger, The unidimensional solidification of a binary eutectic system with a time-dependent surface temperature, ASME J. Heat Transfer 90 (1968) 27–31.
[18] T.R. Goodman, J.J. Shea, The Melting of Finite Slabs, Journal of Applied Mechanics 27 (1) (1960) 16–24, doi:10.1115/1.3643893.
[19] J. Caldwell, Y. Kwan, On the perturbation method for the Stefan problem with time-dependent boundary conditions, International Journal of Heat and Mass Transfer 46 (8) (2003) 1497–1501.
[20] M. Parhizi, A. Jain, Solution of the phase change Stefan problem with time-dependent heat flux using perturbation method, Journal of Heat Transfer 141 (2) (2019).
[21] R. Pedroso, G. Domoto, Perturbation solutions for spherical solidification of saturated liquids, ASME J. Heat Transfer 95 (1973) 42–46.
[22] M. Özışık, S. Guçeri, A variable eigenvalue approach to the solution of phase-change problems, The Canadian Journal of Chemical Engineering 55 (2) (1977) 145–148.
[23] J. Crank, Two methods for the numerical solution of moving-boundary problems in diffusion and heat flow, The Quarterly Journal of Mechanics and Applied Mathematics 10 (2) (1957) 220–231.
[24] R. Furzeland, A comparative study of numerical methods for moving boundary problems, IMA Journal of Applied Mathematics 26 (4) (1980) 411–429.
[25] V. Voller, M. Cross, Accurate solutions of moving boundary problems using the enthalpy method, International journal of heat and mass transfer 24 (3) (1981) 545–556.
[26] R. Bonnerot, P. Jamet, Numerical computation of the free boundary for the two-dimensional Stefan problem by space-time finite elements, Journal of Computational Physics 25 (2) (1977) 163–181.
[27] G. Beckett, J.A. Mackenzie, M. Robertson, A moving mesh finite element method for the solution of two-dimensional Stefan problems, Journal of Computational Physics 168 (2) (2001) 500–518.
[28] R. Viskanta, Heat Transfer During Melting and Solidification of Metals, Journal of Heat Transfer 110 (4b) (1988) 1205–1219, doi:10.1115/1.3250621.
[29] A.K. Singh, A. Kumar, A Stefan problem with variable thermal coefficients and moving phase change material, Journal of King Saud University-Science 31 (4) (2019) 1064–1069.
[30] M.F. Natale, D.A. Tarzia, Explicit solutions to the one-phase Stefan problem with temperature-dependent thermal conductivity and a convective term, International Journal of Engineering Science 41 (15) (2003) 1685–1698.
[31] C. Rogers, P. Broadbridge, On a nonlinear moving boundary problem with heterogeneity: application of a reciprocal transformation, Zeitschrift für angewandte Mathematik und Physik ZAMP 39 (1) (1988) 122–128.
[32] Y. Ruan, B.Q. Li, J.C. Liu, A finite element method for steady-state conduction-advection phase change problems, Finite elements in analysis and design 19 (3) (1995) 153–168.
[33] A.L. Lombardi, D.A. Tarzia, Similarity solutions for thawing processes with a heat flux condition at the fixed boundary, Meccanica 36 (3) (2001) 251–264.
[34] M. Turkyilmazoglu, Stefan problems for moving phase change materials and multiple solutions, International Journal of Thermal Sciences 126 (2018) 67–73.
[35] J. Crank, The mathematics of diffusion, Clarendon Press, Oxford, 1956.
[36] B. Baliga, S. Patankar, A new finite-element formulation for convection-diffusion problems, Numerical Heat Transfer 3 (4) (1980) 393–409.
[37] A. Ogata, R.B. Banks, A solution of the differential equation of longitudinal dispersion in porous media: fluid movement in earth materials, US Geological Survey, Professional Paper 411-A (1961).
[38] W. Gröbner, N. Hofreiter, Integraltafel. Wien, Springer-Verlag, 1949.
[39] M. Parhizi, A. Jain, Eigenfunction-based solution for one-dimensional solid-liquid phase change heat transfer problems with advection, Int. J. Therm. Sci, in review (2021).